

WEAKLY-SUPERVISED MULTI-TASK LEARNING FOR AUDIO-VISUAL SPEAKER VERIFICATION

Anith Selvakumar and Homa Fashandi¹

LG Electronics, Toronto AI Lab

ABSTRACT

In this paper, we present a methodology for achieving robust multimodal person representations optimized for open-set audio-visual speaker verification. Distance Metric Learning (DML) approaches have typically dominated this problem space, owing to strong performance on new and unseen classes. In our work, we explored multitask learning techniques to further boost performance of the DML approach and show that an auxiliary task with weak labels can increase the compactness of the learned speaker representation. We also extend the Generalized end-to-end loss (GE2E) to multimodal inputs and demonstrate that it can achieve competitive performance in an audio-visual space. Finally, we introduce a non-synchronous audio-visual sampling random strategy during training time that has shown to improve generalization. Our network achieves state of the art performance for speaker verification, reporting **0.244%**, **0.252%**, **0.441%** Equal Error Rate (EER) on the three official trial lists of VoxCeleb1-O/E/H, which is to our knowledge, the best published results on VoxCeleb1-E and VoxCeleb1-H.

Index Terms— speaker verification, multimodality, audio-visual, person representation, multi-task learning

1. INTRODUCTION

Human interactivity with artificially intelligent systems continue to gain popularity, especially as devices become capable of advanced tasks and are seamlessly integrated with our daily lives (e.g., digital voice assistants). A critical component to enabling realistic interactions with such systems is speaker verification, the process of identifying whether a spoken utterance belongs to an existing pre-enrolled speaker profile. Applications can range from user authentication to personalized experiences, however, environmental noise and occlusion are only a few of the challenges associated with performing reliable speaker verification in real-world settings [1].

To this end, multimodal systems, which process information from multiple input modalities, have been increasing in popularity due to the potential of added robustness and improved performance [2]. Especially useful in uncontrolled environments, multimodal systems can be designed to be fail-safe against missing or corrupt input modalities with little to no degradation of system performance [3]. For the case of speaker verification, audio and visual signals, in particular have shown improvement in false-reject rates when used in multimodal systems compared to audio-only and visual-only systems [4] [5] [6] [7] [8].

This work explores upon the existing literary work in the space of audio-visual speaker verification, and expands upon it leveraging advanced techniques in multimodal, contrastive, and multi-task

learning. Our main contributions are as follows: (i) Demonstrate that multi-task learning can be used to further enhance the feature representations learned by DML to achieve identity-discriminative and generalizable person representations. (ii) Extend the Generalized End to End Loss (GE2E) [9] from a unimodal to a multimodal input space. (iii) Introduce a multimodal sampling strategy for person representation that shows to improve generalization. These contributions demonstrate SoTA performance with EER of 0.244%, 0.252%, and 0.441% on the VoxCeleb1-O/E/H test splits.

2. BACKGROUND

In this section, we describe relevant works and select technical concepts that are foundational to our work.

2.1. Related Works

Prior studies reveal interesting developments in audio-visual speaker verification. While these works have proposed various architectural improvements and augmentation strategies, a majority use DML training approaches, and in general, devise increasingly complex networks to realize only modest performance gains. For example, Qian et al. [5] introduced a joint learned embedding-level network architecture, trained with their contrastive loss sampling and data augmentation strategy that was originally presented in [8]. Sun et al. [10] implements joint-attention pooling on the audio-visual inputs to enhance the weights of time frames that are most impactful for person representation. Further, Tao et al. [11] cite noisy labels in common large-scale datasets as a limitation to speaker representation learning, and propose a two-step multimodal deep cleansing network to identify noisy samples for removal prior to training.

Our work differs by hypothesizing that DML feature learning can be enhanced by introducing a supervised multi-task component to the objective function. This is on the basis of [12], where it was shown that the features learned through classification and contrastive approaches can differ. Further, rather than dataset cleansing, we hypothesize that noisy labels can be leveraged to achieve more robust speaker representations, and propose noise-tolerant training methods so they can serve as regularization during training for open-set tasks.

2.2. Multimodal Fusion

Multimodal fusion has been achieved through many different techniques [1] [13] [14]. For robustness in non-ideal scenarios in the audio-visual domain, the attention-based fusion network (AFN) [1] proposed for audio-visual person verification is of particular interest. AFN is able to adapt to corrupt or missing modalities by re-weighting the contribution of either modality at time of fusion. This is achieved through an attention mechanism that is extended across the modality axis to obtain modality attention weights:

LG Electronics, Toronto AI Lab, 590 King Street W, Toronto, ON, M5V1M3, Canada. ¹email: [a.selvakumarasingam, homa.fashandi]@lge.com

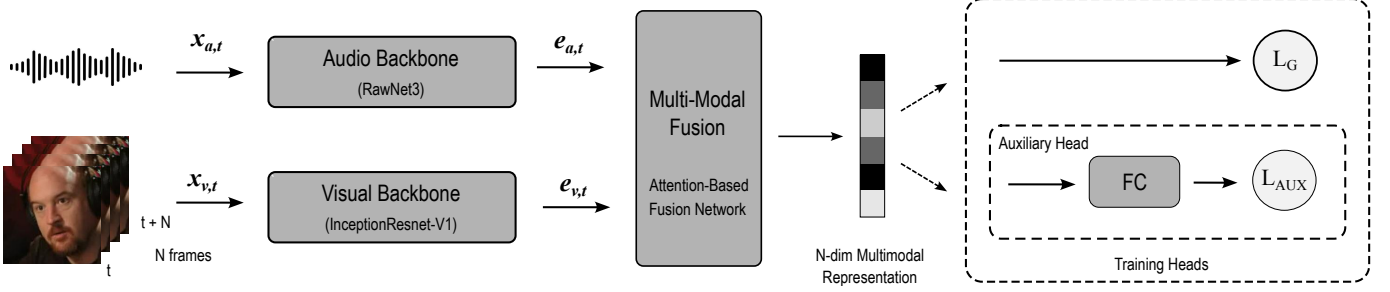


Fig. 1: System level diagram of the REPTAR network. The multimodal representation feeds into the training heads, which are removed during inference time. For inference, the multimodal representation can be used directly for speaker verification

$$\hat{a}_{\{a,v\}} = f_{att}([\mathbf{e}_a, \mathbf{e}_v]) = \mathbf{W}^T [\mathbf{e}_a, \mathbf{e}_v] + \mathbf{b}, \quad (1)$$

where e_a and e_v are transformed audio and visual representations, respectively. Learnable parameters \mathbf{W}^T and \mathbf{b} are optimized during the training process. Modality attention weights are then re-scaled via Softmax to obtain scores between $[0, 1]$ and applied across the embedding axis prior to aggregation to form the fused multimodal representation.

2.3. Generalized End-to-End (GE2E) Loss

The GE2E loss, originally proposed in [9] for audio-based speaker verification, adopts an approach that uses class centroid distances during optimization. Specifically, the loss is calculated from a similarity matrix between each utterance representation embedding to all speaker utterance centroids. From this matrix, a total contrastive loss is calculated based upon positive components (distance between each utterance to its speaker utterance centroid) and a hard negative component (distance between utterance to closest false speaker centroid).

3. ROBUST AUDIO-VISUAL PERSON ENCODER

In this section, we elaborate on our proposed approach to developing a robust audio-visual person encoder.

3.1. Generalized End-to End Multimodal Loss

Large scale datasets often contain noisy labels that can confuse networks during training and limit performance. We, however, propose to leverage these noisy samples to improve generalizability. We hypothesize that using a centroid-based optimization approach, outliers and noisy labels will act as a regularizer during training to lead to better generalization. We achieve this through extending the GE2E loss to a multimodal input space, and refer to this new loss function as GE2E-MM.

The GE2E-MM architecture relies on batching $N \times M$ audio and visual inputs, $x_{\{a,v\},ji}$ ($1 \leq j \leq N, 1 \leq i \leq M$), where N and M are unique speakers and speaker utterances, respectively.

We define the audio-visual latent representation as:

$$\mathbf{e}_{ji} = \frac{f(\mathbf{x}_{a,ji}; \mathbf{x}_{v,ji}; \mathbf{w})}{\|f(\mathbf{x}_{a,ji}; \mathbf{x}_{v,ji}; \mathbf{w})\|_2} \quad (2)$$

where $f(\mathbf{x}_{a,ji}; \mathbf{x}_{v,ji}; \mathbf{w})$ represents the transfer function of the neural network, with $\mathbf{x}_{a,ji}$ and $\mathbf{x}_{v,ji}$ representing raw audio and visual

inputs; and \mathbf{w} representing the network weights. Using this, a similarity matrix, $S_{ji,k}$, of scaled cosine similarities is computed, representing a similarity metric between each multimodal embedding e_{ji} and each speaker centroid, c_k , from the $N \times M$ batch:

$$\mathbf{c}_k = \frac{1}{M} \sum_{m=1}^M \mathbf{e}_{km} \quad (3)$$

$$S_{ji,k} = w \cdot \cos(\mathbf{e}_{ji}, \mathbf{c}_k) + b \quad (4)$$

where w and b are learnable parameters. Using this similarity matrix a contrastive loss is calculated for each multimodal representation, e_{ji} , focusing primarily on all positive pairs and a hard negative pair. The GE2E-MM loss, \mathcal{L}_G , is then defined as:

$$\mathcal{L}_G(\mathbf{S}) = \sum_{j,i} \mathcal{L}(\mathbf{e}_{ji}) \quad (5)$$

where,

$$\mathcal{L}(e_{ji}) = 1 - \sigma(S_{ji,j}) + \max_{\substack{1 \leq k \leq N \\ k \neq j}} \sigma(S_{ji,k}) \quad (6)$$

where σ represents the sigmoid function. Optimization of Equation 6 has the effect of pushing embeddings from identical speakers towards its respective centroid, and away from its closest dissimilar speaker centroid.

3.2. Multi-Task Objective Function

We hypothesize that adding an age classification task will force more subtle characteristics to be extracted from the inputs and embedded in the multimodal representation. With this auxiliary task, we can define a multi-task loss function:

$$\mathcal{L}_{MTL} = \gamma \cdot \mathcal{L}_G(S) + (1 - \gamma) \cdot \mathcal{L}_{AUX}, \quad (7)$$

where γ is a scalar weight that is applied in order to balance the losses and prevent one task from dominating. The parameter is obtained through hyper-parameter tuning. \mathcal{L}_G and \mathcal{L}_{AUX} are GE2E-MM and auxiliary task losses, respectively.

3.3. Unsynchronized Audio-Visual Random Sampling

Audio and visual samples sourced from the same utterance can be highly correlated on speaker-irrelevant features [15] [16]. This can limit the learning of distinctive features and instead cause the training to focus on peripheral attributes such as noise or environmental factors. To prevent this, we propose a random sampling strategy

where audio and visual samples are separately extracted from different utterances from the same speaker and combined into an unsynchronized audio-visual pair before being passed into the network.

Using the AFN for audio-visual fusion, we implemented the above-mentioned developments to form the end-to-end encoder network: ‘Robust Encoder for Persons through Learned Multi-Task Representations’ (REPTAR), shown in Figure 1.

4. EXPERIMENTATION

This section describes the methodology used to achieve the results that are reported in this work.

4.1. Setup

4.1.1. Dataset and Preprocessing

VoxCeleb is a large-scale audio-visual dataset collected from open-source media for speaker recognition and is widely used in literature. For our experimentation, VoxCeleb2 [17] was used for training, while pre-defined test splits from VoxCeleb1 [18] for evaluation.

During pre-processing, utterance video files were decomposed into face tracks at a 1 frame per second (FPS) rate and re-scaled to 160×160 pixels, and voice track that was cropped to a random window size between 4-8 seconds. For evaluation, utterances were sourced from the predefined test splits. Voice clips was limited to a fixed 4 second window with a random onset time and faces are extracted from the same utterance.

4.1.2. Voice and Face Representation

Pre-trained encoders was used to obtain voice and face representations. For voice profiles, RawNet3, proposed in [19] was used. RawNet3 was trained on the VoxCeleb2 dataset and evaluated on the VoxCeleb1-O test split and demonstrates competitive EER performance. For face representation, the InceptionResnet-V1 architecture [20] was used, which was pre-trained on the VGGFace2 [21] dataset. VGGFace2 was confirmed to have a negligible overlap between the test set (5 out of 1251 speakers), which was verified to play no impact to the model performance when rounded to three significant figures.

4.1.3. Fusion Strategy and Training Details

For our implementation of the AFN, the 512 dimension face embedding and 256 dimension voice embedding obtained from their pre-trained models are L2 normalized and transformed independently into a 512 dimension space for equal representation prior to fusion. This transformation consists of two linear layers, with a ReLU activation and batch normalization layer in between. The attention layer is implemented as a linear layer with input size 1024 and output of 2 to represent the modality scores. These softmaxed scores are applied as multiplicative factors to the transformed representations, which are then concatenated to form the multimodal representation.

This network was trained on a Tesla V100 GPU. Batch sizes was set to 64 with 10 utterances per speaker. The Adam optimizer [22] was used with an exponentially decaying learning rate, initially set to 0.05 and decaying at a factor of 0.9 per epoch. Early stopping with a patience of 5 epochs was used to prevent overfitting. Multiple seeds were tested to demonstrate reproducibility of results.

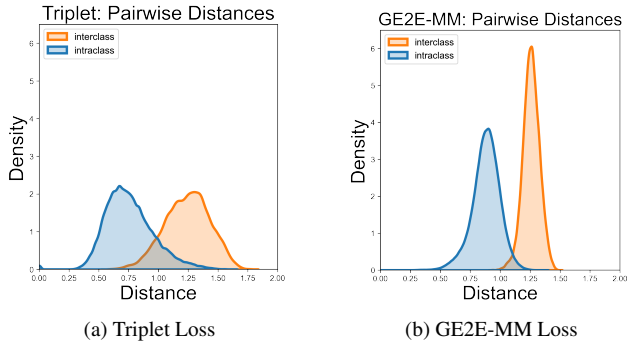


Fig. 2: Interclass and Intra-class Pairwise Distance Distribution of Triplet and GE2E-MM models for a random speaker.

Table 1: Quality of encoded person representation clusters against triplet loss and GE2E-MM loss (with and without auxiliary task)

Clustering Metric	$\mathcal{L}_{triplet}$	$\mathcal{L}_{GE2E-MM}$	
		NoAux	Aux
Silhouette Coefficient [24] (\uparrow)	0.233	0.501	0.504
Calinski-Harabasz Score [25] (\uparrow)	4541	6264	6454
Davies-Bouldin Score [26] (\downarrow)	1.4657	0.8613	0.8599

4.1.4. Auxiliary Task

An age prediction auxiliary task was implemented to enhance feature learning during training. The task head consisted of two linear layers with a ReLU activation and batch normalization layer in between. A sigmoid layer was used at the end of the network to represent normalized age predictions. Mean-squared error loss was used as the objective function. The optimal γ value in the compound loss function of Equation 7 was determined to be 0.015 through hyperparameter tuning.

Age labels were obtained from the AgeVoxCeleb dataset [23], which contain estimated ages for approximately 5000 of 6112 speakers of the VoxCeleb2 dataset. These labels can be considered weak due to label inaccuracies and incompleteness.

4.2. Evaluation

In order to evaluate the performance of the speaker verification system, the Equal Error Rate (EER) metric was calculated for each of the VoxCeleb1 test splits. The EER corresponds to the error rate at which the False Positive Rate (FPR) and False Negative Rates (FNR) are equal, and is a standard metric used for speaker verification [18].

4.3. Results and Ablation Studies

We performed extensive ablation studies to study the effect of each of the proposed strategies. This section describes the results obtained from these studies, along with a comparison to other relevant works.

4.3.1. Effect of the GE2E-MM Loss:

The impact of the GE2E-MM loss was analyzed by studying the encoded audio-visual representations of speaker utterances from identical networks that differed only on the objective function they

Table 2: Ablation Study showing the effect of proposed loss function and auxiliary task on EER.

Loss Function	Aux Task	VC1-O	VC1-E	VC1-H
Triplet [27]	N	6.85	9.57	5.16
GE2E-MM	N	0.323	0.292	0.507
GE2E-MM	Y	0.244	0.252	0.441

Table 3: EER of REPTAR in the presence of corrupted and missing modalities on the VoxCeleb1-O test split

Architecture	Audio Input	Visual Input	EER
REPTAR	<i>clean</i>	<i>clean</i>	0.24
	<i>corrupt</i>	<i>clean</i>	1.98
	<i>missing</i>	<i>clean</i>	1.12
	<i>clean</i>	<i>corrupt</i>	6.12
	<i>clean</i>	<i>missing</i>	1.64

were trained on (GE2E-MM or Triplet [27]). Intra-class pairwise Euclidean distances were measured between all combinations in the set of utterance encodings obtained from the same speaker. Similarly, interclass pairwise distances were measured as the Euclidean distance between the reference speaker’s encoded utterance *centroid* with that of the utterance centroid for every other speaker in the set.

The intra-class and interclass sample distributions for the triplet loss and GE2E-MM loss models are shown in Figure 2. Results show significant reduction in the overlap between intra-class and interclass distributions on the GE2E-MM loss trained network, implying more compact person representations. To validate this further, we employ the Silhouette coefficient [24], Calinski-Harabasz score [25], and the Davies-Bouldin score [26] on the entire test set. The measured result is shown in Table 1. For all three metrics, the values measured by the GE2E-MM loss trained model show improvement against the triplet loss trained model.

4.3.2. Effect of the Auxiliary Task:

The results in Table 1 show the improvement of cluster quality when comparing to the same network trained without the additional task loss. This sentiment is echoed in the results of Table 2, showing approximately 24.5%, 13.7%, and 13.0% EER improvement on the VoxCeleb1-O/E/H test splits. We believe that the auxiliary task of age classification ensured that distinctive markers from both modalities are preserved in the multimodal representation to help generalization and improve overall performance.

4.3.3. Effect of Corrupted and Missing Modality:

Measuring robustness to non-ideal situations was performed by recreating absent or corrupt modalities. An absent modality was emulated by setting the input to zero. Corrupt inputs were emulated using additive white Gaussian noise (AWGN), with $\mu = 0$ and $\sigma_v = [0, 255]$ or $\sigma_a = [-1, 1]$, where μ and σ are mean and standard deviation, respectively. This methodology is consistent with existing literary works [1].

The results in Table 3 show that the multimodal network is robust to missing or corrupt inputs without significantly compromising performance. This can be compared to other architectures that rely

Table 4: Proposed model EER performance compared to SoTA. Lower value signifies a better result. Best results are in **bold**

Architecture	Modality	VC1-O	VC1-E	VC1-H
Chen et al [8]	A	2.308	2.234	3.782
	V	2.260	1.542	2.374
	AV	0.585	0.427	0.735
Qian et al [5]	A	1.622	1.751	3.159
	V	3.042	2.178	3.234
	AV	0.558	0.441	0.793
Sun et al [10]	A	0.99	1.24	2.27
	V	1.44	1.28	2.14
	AV	0.18	0.26	0.49
REPTAR	A	1.64	1.12	1.85
	V	1.12	1.19	1.82
	AV	0.244	0.252	0.441

on both modalities to be present, a constraint that is not always feasible in real-world scenarios.

4.3.4. Effect of Unsynchronized Audio-Visual Random Sampling:

By randomizing the visual and audio inputs within a speaker identity, we were able to see a 22% improvement in performance compared to a model trained using audio and visual inputs from the same utterance. Similar to the findings of Nagrani et al. [16] on disentangled linguistic content and speaker identity yielding better generalization, we believe our improvement is also as result of minimizing mutual information, but between the speaker audio-visual input space.

4.3.5. Summary of Results

REPTAR achieves competitive performance against the previous state of the art, yielding best published results in 7 of 9 test configurations, with an average EER improvement of 12.2%. Results are shown in Table 4 along with a comparison to related works. The results of Tao et al. [11] was omitted due to train-test contamination.

Our proposed model is able to achieve SoTA performance on all test configurations of the VoxCeleb1-E and VoxCeleb1-H test splits, which are considerably larger and target different demographics compared to the VoxCeleb1-O split. Jointly, VoxCeleb1-E and VoxCeleb1-H can be used to describe the REPTAR’s generalizability and quality of feature extraction. The results show that REPTAR goes beyond encoding basic high-level features such as nationality and gender in the representation space, and is able to extract features that can be used to distinguish between even the most similar of speakers.

5. CONCLUSION

In this paper we explored how MTL can be used to enhance representation learning from traditional DML approaches. We demonstrate this through measuring the quality of learned speaker representations trained with an auxiliary task with weak labels. We also show how to leverage noisy labels for regularization in open-set tasks by introducing the GE2E-MM loss. Finally, we show that unsynchronized multimodal random sampling can be used to improve generalization for audio-visual systems. A comprehensive study of MTL task selection and optimized task weighting strategies is left as future work.

6. REFERENCES

- [1] Suwon Shon, Tae Hyun Oh, and James Glass, “Noise-tolerant Audio-visual Online Person Verification Using an Attention-based Neural Network Fusion,” *IEEE International Conference on Acoustics, Speech and Signal Processing (ICASSP)*, 2019.
- [2] Yu Huang, Chenzhuang Du, Zihui Xue, Xuanyao Chen, Hang Zhao, and Longbo Huang, “What Makes Multi-modal Learning Better than Single (Provably),” *Advances in Neural Information Processing Systems*, 2021.
- [3] Aggelos K. Katsaggelos, Sara Bahaadini, and Rafael Molina, “Audiovisual Fusion: Challenges and New Approaches,” *Proceedings of the IEEE*, pp. 1635–1653, 2015.
- [4] Bowen Shi, Abdelrahman Mohamed, and Wei Ning Hsu, “Learning Lip-Based Audio-Visual Speaker Embeddings with AV-HuBERT,” *Proceedings of the Annual Conference of the International Speech Communication Association, INTERSPEECH*, 2022.
- [5] Yanmin Qian, Zhengyang Chen, and Shuai Wang, “Audio-Visual Deep Neural Network for Robust Person Verification,” *IEEE/ACM Transactions on Audio Speech and Language Processing*, 2021.
- [6] Leda Sari, Kritika Singh, Jiatong Zhou, Lorenzo Torresani, Nayan Singhal, and Yatharth Saraf, “A multi-view approach to audio-visual speaker verification,” *IEEE International Conference on Acoustics, Speech and Signal Processing (ICASSP)*, 2021.
- [7] Ruijie Tao, Rohan Kumar Das, and Haizhou Li, “Audio-visual speaker recognition with a cross-modal discriminative network,” *Proceedings of the Annual Conference of the International Speech Communication Association, INTERSPEECH*, 2020.
- [8] Zhengyang Chen, Shuai Wang, and Yanmin Qian, “Multimodality matters: A performance leap on voxceleb,” *Proceedings of the Annual Conference of the International Speech Communication Association, INTERSPEECH*, 2020.
- [9] Li Wan, Quan Wang, Alan Papir, and Ignacio Lopez Moreno, “Generalized end-to-end loss for speaker verification,” *IEEE International Conference on Acoustics, Speech and Signal Processing (ICASSP)*, 2018.
- [10] Peiwen Sun, Shanshan Zhang, Zishan Liu, Yougen Yuan, Tao-tao Zhang, Honggang Zhang, and Pengfei Hu, “Learning Audio-Visual embedding for Person Verification in the Wild,” *arXiv preprint arXiv:2209.04093*, 2022.
- [11] Ruijie Tao, Kong Aik Lee, Zhan Shi, and Haizhou Li, “Speaker recognition with two-step multi-modal deep cleansing,” *IEEE International Conference on Acoustics, Speech and Signal Processing (ICASSP)*, 2023.
- [12] Konstantin Kobs, Michael Steininger, Andrzej Dulny, and Andreas Hotho, “Do Different Deep Metric Learning Losses Lead to Similar Learned Features?,” *Proceedings of the IEEE International Conference on Computer Vision*, 2021.
- [13] Akira Fukui, Dong Huk Park, Daylen Yang, Anna Rohrbach, Trevor Darrell, and Marcus Rohrbach, “Multimodal compact bilinear pooling for visual question answering and visual grounding,” *Conference on Empirical Methods in Natural Language Processing (EMNLP)*, 2016.
- [14] John Arevalo, Tamar Solorio, Manuel Montes-Y-Gómez, and Fabio A. González, “Gated multimodal units for information fusion,” *5th International Conference on Learning Representations, ICLR 2017 - Workshop Track Proceedings*, 2019.
- [15] Sung Hwan Mun, Min Hyun Han, Minchan Kim, Dongjune Lee, and Nam Soo Kim, “Disentangled speaker representation learning via mutual information minimization,” *arXiv preprint arXiv:2208.08012*, 2022.
- [16] Arsha Nagrani, Joon Son Chung, Samuel Albanie, and Andrew Zisserman, “Disentangled Speech Embeddings Using Cross-Modal Self-Supervision,” *IEEE International Conference on Acoustics, Speech and Signal Processing (ICASSP)*, 2020.
- [17] Joon Son Chung, Arsha Nagrani, and Andrew Zisserman, “VoxCeleb2: Deep speaker recognition,” *Proceedings of the Annual Conference of the International Speech Communication Association, INTERSPEECH*, 2018.
- [18] Arsha Nagrani, Joon Son Chung, and Andrew Zisserman, “VoxCeleb: A large-scale speaker identification dataset,” *Proceedings of the Annual Conference of the International Speech Communication Association, INTERSPEECH*, 2017.
- [19] Jee Weon Jung, You Jin Kim, Hee Soo Heo, Bong Jin Lee, Youngki Kwon, and Joon Son Chung, “Pushing the limits of raw waveform speaker recognition,” *Proceedings of the Annual Conference of the International Speech Communication Association, INTERSPEECH*, 2022.
- [20] Christian Szegedy, Sergey Ioffe, Vincent Vanhoucke, and Alexander A. Alemi, “Inception-v4, inception-ResNet and the impact of residual connections on learning,” *31st AAAI Conference on Artificial Intelligence, AAAI 2017*, 2017.
- [21] Qiong Cao, Li Shen, Weidi Xie, Omkar M. Parkhi, and Andrew Zisserman, “VGGFace2: A dataset for recognising faces across pose and age,” *13th IEEE International Conference on Automatic Face and Gesture Recognition*, 2018.
- [22] Diederik P Kingma and Jimmy Lei Ba, “ADAM: A Method for Stochastic Optimization,” *International Conference on Learning Representations*, 2015.
- [23] Naohiro Tawara, Atsunori Ogawa, Yuki Kitagishi, and Hosana Kamiyama, “Age-VOX-Celeb: Multi-Modal Corpus for Facial and Speech Estimation,” *IEEE International Conference on Acoustics, Speech and Signal Processing (ICASSP)*, 2021.
- [24] Peter J. Rousseeuw, “Silhouettes: A graphical aid to the interpretation and validation of cluster analysis,” *Journal of Computational and Applied Mathematics*, 1987.
- [25] T. Calinski and J. Harabasz, “A dendrite method for cluster analysis,” *Communications in Statistics*, vol. 3, no. 1, pp. 1–27, 1974.
- [26] David L. Davies and Donald W. Bouldin, “A cluster separation measure,” *IEEE Transactions on Pattern Analysis and Machine Intelligence*, vol. PAMI-1, no. 2, pp. 224–227, 1979.
- [27] Florian Schroff, Dmitry Kalenichenko, and James Philbin, “FaceNet: A unified embedding for face recognition and clustering,” *Proceedings of the IEEE Computer Society Conference on Computer Vision and Pattern Recognition*, 2015.